Characterization of Flaws in a Tube Bundle Mock-Up for Reliability Studies*

by

D. S. Kupperman and S. Bakhtiari

Argonne National Laboratory
Argonne, IL 60439

October 1996

DISCLAIMER

INVITED PAPER for presentation at the 24th Water Reactor Safety Meeting, October 21-23, 1996, Bethesda, MD.

*Work supported by the Office of Nuclear Regulatory Research, U.S. Nuclear Regulatory Commission.

Characterization of Flaws in a Tube Bundle Mock-Up for Reliability Studies

D. S. Kupperman and S. Bakhtiari

Argonne National Laboratory

Abstract

As part of an assessment of in-service inspection of steam generator tubes, we will assemble a steam generator mock-up for round robin studies and use as a test bed in evaluating emerging technologies. Progress is reported on the characterization of flaws that will be part of the mock-up. Eddy current and ultrasonic techniques are being evaluated as a means to characterize the flaws in the mock-up tubes before final assembly. Twenty Inconel 600 tubes with laboratory-grown cracks, typical of those to be used in the mock-up, were provided by Pacific Northwest National Laboratory for laboratory testing. After the tubes were inspected with eddy current and ultrasonic techniques, they were destructively analyzed to establish the actual depths, lengths, and profiles of the cracks. The analysis of the results will allow the best techniques to be used for characterizing the flaws in the mock-up tubes.

Background

There is a need to provide experimental data and predictive correlations and models to permit the U.S. Nuclear Regulatory Commission (NRC) to independently evaluate the integrity of steam generator (SG) tubes as plants age and degradation proceeds, new forms of degradation appear, and new defect-specific management schemes are implemented. One key area to be addressed to help meet those needs is the assessment of procedures and equipment used for in-service inspection (ISI) of SG tubes. As part of the assessment of in-service inspection of SG tubes, a steam generator mock-up will be used for round robin (RR) studies using currently practiced techniques and as a test bed for evaluating emerging technologies. The mock-up will contain several hundred tube openings and will include a variety of flaws and artifacts.

Eddy current (EC) and ultrasonic techniques (UT) are being evaluated as means to characterize the defects in the mock-up tubes before final assembly. Twenty Inconel 600 tubes with laboratory-grown cracks were provided by Pacific Northwest National Laboratory (PNNL) for laboratory testing. After the tubes were inspected with EC and UT techniques, they were destructively examined to establish the actual depths, lengths, and profiles of the cracks. Analysis of the results will allow the best techniques to be used for characterization of flaws in the mock-up tubes.

The 20 tube specimens were a subset of tubes prepared under laboratory conditions by the Westinghouse Science and Technology Center under a subcontract with PNNL. The specimens exhibit longitudinal inner-surface stress corrosion cracks (LIDSCC), longitudinal outer-surface stress corrosion cracks (LODSCC), circumferential inner-surface stress corrosion cracks (CIDSCC), circumferential outer-surface stress corrosion cracks (CODSCC), and intergranular attack (IGA). Nine of the tubes show a roll transition. The Inconel 600 tubes are ≈0.30 m (12 in.) long, 22.2 mm (0.875 in.) in diameter, and have a wall thickness of 1.27 mm (0.050 in.). The tubes were subjected to ultrasonic depth and length characterization by high-frequency diffraction, Lamb wave, and amplitude drop methods. Eddy current depth and length were estimated by using a rotating pancake coil (RPC), multicoil arrays, a Zetec Plus Point probe, and multiparameter EC data analysis using neural network algorithms.

Tubes were ultrasonically inspected at the Idaho National Engineering Laboratory (INEL) to help determine the optimal method for inspecting tubes before they are integrated into the SG mock-up. High-frequency, longitudinal, and shear waves in a focused, pulse echo mode were used with waves incident at 0 and 45° (for both axial and circumferentially oriented cracks). All of the PNNL/INEL inspections were carried out from the outside of the tube. High-frequency backscatter and frequency analysis was used to characterize IGA. A, B, and C scans were used to characterize all of the cracks and the IGA. Time-of-flight (TOF) data were used to estimate depth when a crack tip echo was detectable, otherwise a 14-dB drop method with signal movement was used to estimate depth. Frequencies of 20-50 MHz were employed in an immersion tank. However, because of the attenuation in Inconel 600, the peak in the frequency spectrum is ≈30 MHz for propagation through the thickness and back (in pulse echo mode). Two calibration tubes were used. The first tube contained two sets of outer-surface saw cuts. The first set included four axial cuts 0.25-1.02 mm (0.010-0.040 in.) deep and 5.08-9.78 mm (0.200-0.385 in.) long. The second set contained five circumferential cuts 0.127-1.016 mm (0.005-0.040 in.) deep and 2.16-6.86 mm (0.085-0.270 in.) long. A second tube contained outer-surface saw cuts (axial and circumferential) and

electro-discharge machining (EDM) notches on the inner and outer surfaces. The saw cuts are 0.25-1.02 mm (0.010-0.040 in.) deep and 3.43-9.53 mm (0.135-0.375 in.) long. The EDM notches are nominally 0.51 mm (0.020 in.) deep and 6.35 mm (0.250 in.) long.

Samples were also inspected at ASEA Brown-Boveri (ABB) AMDATA with an ultrasonic probe that propagated Lamb waves in the tube wall, which are unaffected by a roll transition. These waves propagate in a free tube wall and are capable of detecting inner- or outer-surface circumferential cracks. Although axial cracks are not detectable with this probe unless circumferentially oriented branches are present, in principle, it is possible to make a Lamb wave probe that could detect axial cracks. The probe for the data reported in this paper is used in a scan mode that covers a range of 140 mm (5.5 in.). In general, not enough information is present in the Lamb wave echo signal to determine the depth, but general estimates can be made by measuring the echo amplitude. Defect length is accurately estimated by observing the drop in signal amplitude as the defect is scanned. IGA can be called correctly because the echo signals are generated over a large area of the tube. Calibration was carried out with a tube that contained circumferential EDM notches with through-wall depths of 20, 40, and 60% and arc lengths of 20, 40, and 60°. The signal from the 20% TW, 60 degree arc notch was set to 80% full screen height. The probe was moved axially 1.3 mm (0.05 in.) for every 360° scan. A, B, and C scans were generated. The probe was operated at a frequency of approximately 5 MHz. A PC-based Intraspect ultrasonic system was used to collect the data.

The tubes were also inspected with an EC C5/HD array probe at Atomic Energy of Canada, Ltd. (AECL). The probe consists of three parts, two of which contain differential transmit-receive (TR) pancake coil arrays, while the third contains a bobbin coil that was used simultaneously in differential and absolute modes. Each pancake array consisted of eight independent TR units. The coils in the two arrays are rotated relative to each other to completely cover the entire circumference. Thus, each unit "sees" an arc of 22.5°. The sensitivity to axial and circumferential cracks was comparable. Data could be displayed in Zetec Eddynet C-scan and clip-plot formats. The data from the absolute channels of the bobbin coil were useful in detecting long axial cracks. The amplitude from the bobbin coil was useful in distinguishing axial cracks from IGA. Eddy current (EC) data presented in this report were collected with a Zetec MIZ-30 interfaced with a Hewlett Packard 700 series workstation. Data acquisition and analysis were carried out with Zetec Eddynet software. A standard Zetec 4D probe driver with Zetec PM-1 motor controller was used to pull the probe through the tube at a constant speed of 0.30 m/s (12 in./s). Calibration was carried out with a standard ASME tube, a tube supplied by PNNL that contained axial and circumferential outer-surface notches, and a Westinghouse-supplied calibration tube containing a 20% outer-surface axially symmetric EDM notch, a dent, and 1.6-mm (0.060-in.)-diameter through-wall holes. Lack of calibration tubes with inner-surface notches and limited outer-surface notches somewhat limited the ability to estimate the depth of the cracks. Data were collected as the probe was pulled back through the specimen and then through the calibration tubes. The frequencies used were 45, 90, 180, and 400 kHz. The dent was used to adjust the phase angle while the dent signal was oriented horizontally. The vertical component of the 20% outer-surface notch groove signal was set to 10 V. Frequency dependence of the Lissajous figure orientation and of the vertical component of the signal amplitude were used to distinguish outer-surface from inner-surface flaws and to determine whether the defect was deep or shallow. The expansion transition caused some problems with signal interpretation. If a flaw was detected with the array but not with the bobbin coil, it was called circumferential. If the flaw was detected by both array and bobbin coil, it was identified as axial or IGA.

Using a pancake coil, we conducted a neural-network analysis of the multiparameter (four frequency) EC data collected for the 20 tubes (C. V. Dodd formerly of Oak Ridge National Laboratory)[1,2]. The EC coils were ≈4.6 mm (0.180 in.) in diam. Data were acquired with the standard Zetec MIZ-30 acquire program. Training of the neural net was previously carried out with tube standards and 23 samples with flaws having a somewhat different morphology. These samples also had axial and circumferential outer-surface stress corrosion cracks and IGA that were metallographically sectioned. A complication in this effort was a lack of training data for inner-surface defects and only one training sample with a roll transition. Standards used contained 360° circumferential notches 20, 40, 60, and 80% throughwall. Lift off of 0.1 and 0.2 mm (0.004 and 0.008 in.) was also part of the calibration tube and was used to set the phase shift so the lift-off signal is horizontal. The standard also contained a 100%-deep groove and axial notches.

Results

Figure 1 shows estimated crack depth determined by high-frequency ultrasonic-wave examination and by a neural-network algorithm applied to multiparameter EC data from a pancake coil vs. the maximum crack depth determined by metallographic analysis of the tubes.

The UT technique overestimates the depth of the crack in most cases, especially for the shallow cracks. The main problem for the ultrasonic interrogation was the difficulty in detecting the echo from the crack

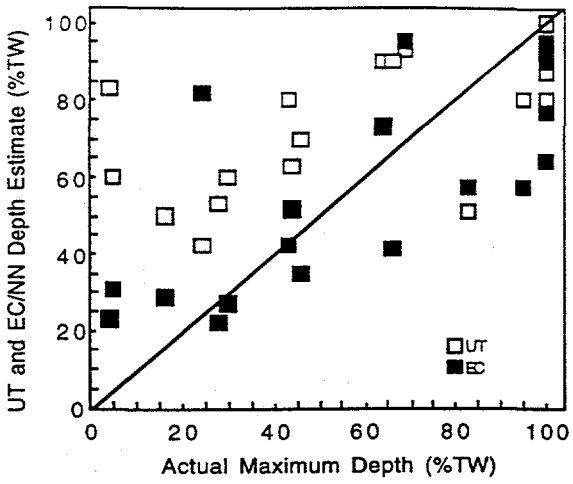

Fig.1. Comparison of estimated depth (PNNL/INEL) using high frequency ultrasonic waves (open squares) and estimated depth from a neural network algorithm applied to EC data (black squares) vs. the maximum depth of crack from metallographic analysis (PNNL) of set of 20 SG tube specimens.

tip that is used to obtain the depth estimate. The results from neural network analysis of EC data are better and are particularly encouraging, because a proper training data set was not available for this analysis. Significant improvements in the correlation are expected when optimized training sets are used with this neural network algorithm. UT and EC neural-network results are compared in Fig. 2. The depth estimated by the UT technique is consistently greater than that predicted by the neural-network algorithm applied to the EC data.

To better understand the problems encountered while estimating depths, data from the 20 tubes have been analyzed in several ways. The data presented in Fig. 3 present the results of depth predictions for tubes with and without a roll transition. No dramatic difference in depth-measuring capability can be observed when using the neural network algorithm and EC data.

Some estimates of flaw depth were also made with an ultrasonic probe from the inner surface of the tube (PNNL/Westinghouse evaluation of tubes). The estimated depth from the inner surface are, on the average, noticeably lower than those from the outer surface. This difference could be the result of differences in probe design but may also be the result of tube curvature effects. Waves incident on the tube inner wall are somewhat focused, whereas waves incident on the outer surface are spread out as they enter the tube wall. Ultrasonic and EC results are presented in Fig. 4.

The results of applying a neural network algorithm to EC data are presented as a function of flaw type in Fig. 5. Preliminary estimates from longitudinal outer- and inner-surface cracks, circumferential outer- and inner-surface cracks, and IGA are separated. No single defect appears significantly easier to characterize than any other, although the correlation coefficient from a linear fit to data restricted to outer surface axial and circumferential cracks is a respectable 0.9 (otherwise it is 0.73 for all data). This result emphasized the success possible with neural network analysis of data if proper training set data are available. However, the result was limited to a small data set and when upper and lower 95% confidence limits are calculated, the need for larger data sets to judge the effectiveness of neural net analysis becomes apparent. The upper and lower confidence limits for the mean and individual (i.e., additional) points can be seen for OD defects in Fig. 6. The range of upper and lower confidence limits is rather large. For example, if a new point were added to the data for an actual maximum depth of 50%, there is a 95% probability that the estimated depth will fall between 15 and 75%, while the mean will still lie between 35 and 55%.

Analysis of EC data from the 20 tube set also includes a phase shift analysis of Plus Point data carried out at Argonne with Zetec Eddynet95 software on data collected at Zetec. Phase analysis was used to estimate the depth of cracks. Calibration was carried out with a series of EDM notches in calibration tubes. The results are reasonable, particularly if restricted to the cracks that are not IGA. Figure 7 shows the results of the analysis of Plus Point data compared to destructive examination. The correlation coefficient is about 0.75 for a linear fit to all the data with especially good results for the ID cracks. Figure 8 shows Plus Point data with 95% confidence limits. Again, the range of the upper and lower confidence limits is very large because of the small size of the data set.

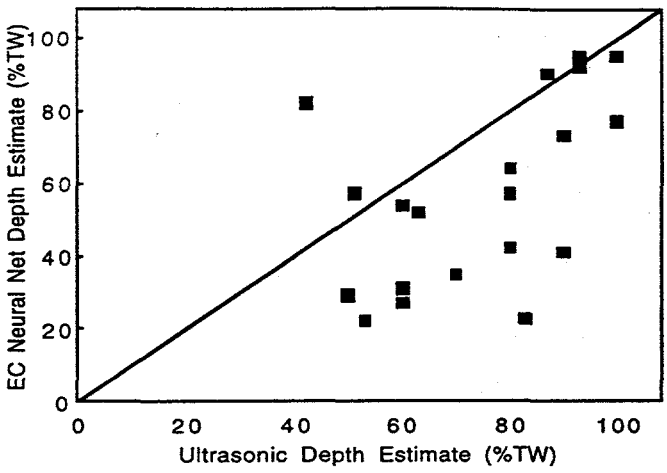

Fig. 2. Comparison of flaw depth estimates from high-frequency ultrasonic wave technique (PNNL/INEL) and neural network algorithm applied to eddy current data.

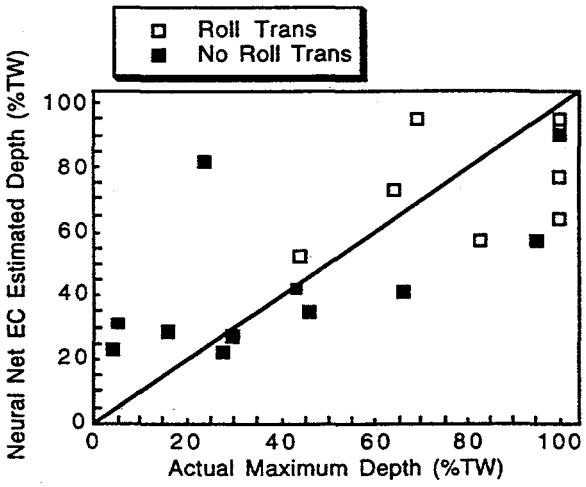

Fig. 3. Comparison of estimated depth applying neural network algorithm to eddy current data for tubes with and without roll transition.

A comprehensive characterization of crack length was also carried out with the Zetec Plus Point probe. Crack lengths estimated from the data are compared with destructive examination (DE) carried out by PNNL. The data were acquired at Zetec and then analyzed at Argonne with Eddynet95 software in the c-scan mode; the results are shown in Fig. 9. For complicated crack structures revealed by DE, the full extent of cracking was compared to the estimated length. If a well-defined deep crack was found among a series of shallow cracks, the length of the deep crack was compared to the EC-determined length. The results for circumferential cracks (0.99 linear fit correlation coefficient [LFCC]) are better than for axial cracks (0.90 LFCC). Defining the ends of the crack is difficult because the EC signal does not end sharply. Subjective judgment is therefore required in estimated circumferential or axial crack lengths. The length of inner wall cracks may be much easier to determine than those of outer wall cracks because the eddy current signal is defined better (0.99 LFCC for ID cracks versus 0.92 LFCC for OD cracks).

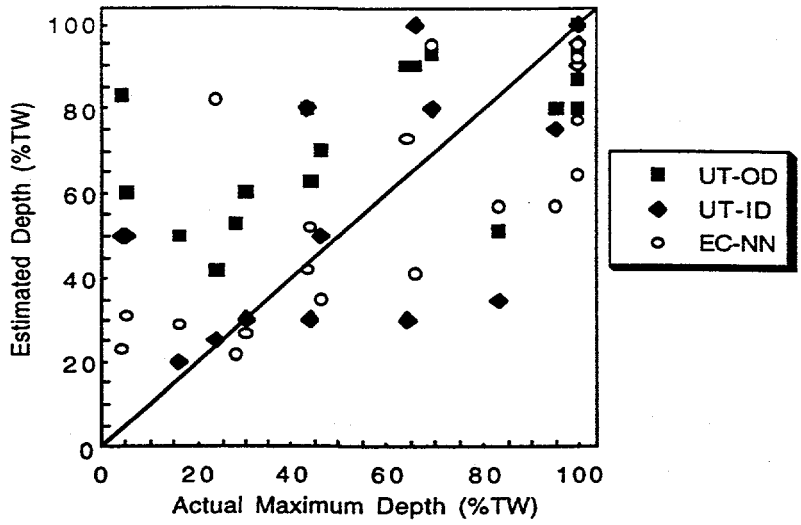

Fig. 4. Estimates of crack depth obtained by ultrasonic wave inspection of inner (Westinghouse/ PNNL) and outer (PNNL/INEL) surfaces of 20 tubes, along with neural network EC results vs. actual maximum depth.

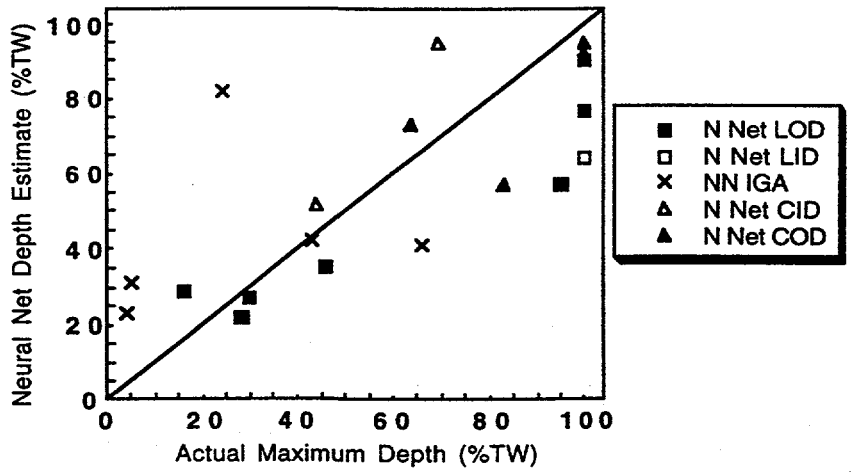

Fig. 5. Results of applying neural network algorithm to eddy current data as a function of longitudinal OD cracks, longitudinal ID cracks, circumferential OD cracks, circumferential ID cracks, and IGA.

An alternative to characterizing crack lengths with eddy currents is the use of ultrasonic techniques. One possibility is to use ultrasonic guided or Lamb waves launched from the inside of the tube and propagating axially in the tube wall. An ultrasonic Lamb wave image (from ABB-AMDATA) of the laboratory-grown CODSCC in one of the Inconel 600 steam generator tubes is shown in Fig. 10. This image suggests six crack segments, five at the same axial location and one offset axially with an arc length of 50°. Total arc length indicated ultrasonically is 130°. The destructive analysis (by PNNL) showed a crack with a total arc length of

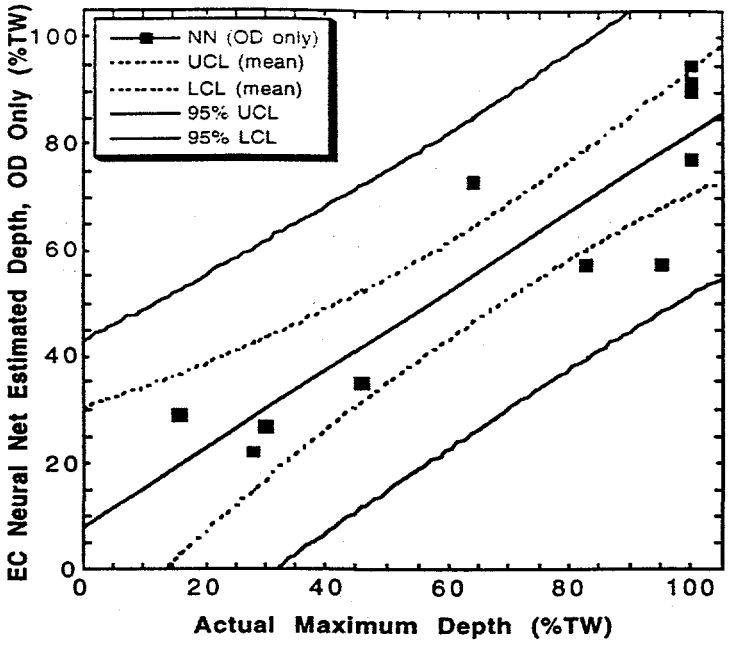

Fig. 6. Upper and lower 95% confidence limits for mean and individual (i.e., additional) points for depth estimates determined by neural network analysis (OD defects only).

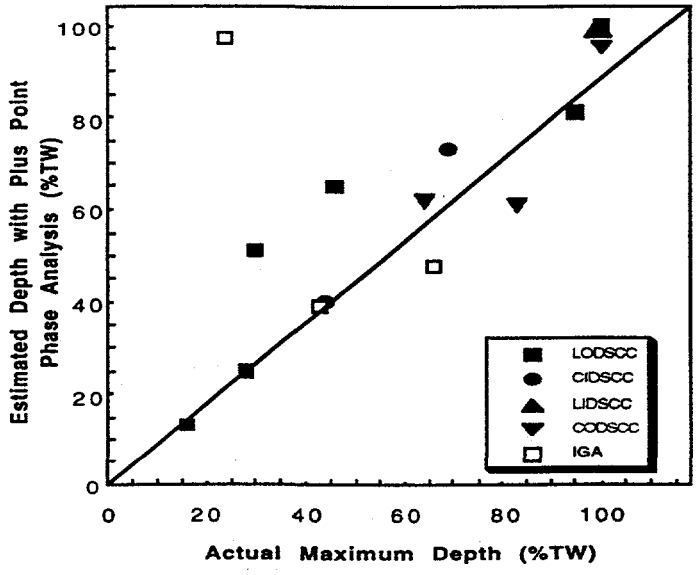

Fig. 7. Crack depth estimates from eddy current data from 20-tube set and phase shift analysis of Plus Point data. Analysis was carried out at Argonne with Eddynet95 software. Calibration used a series of EDM notches in calibration tubes. Correlation coefficient is ≈0.75 for a linear fit to all data.

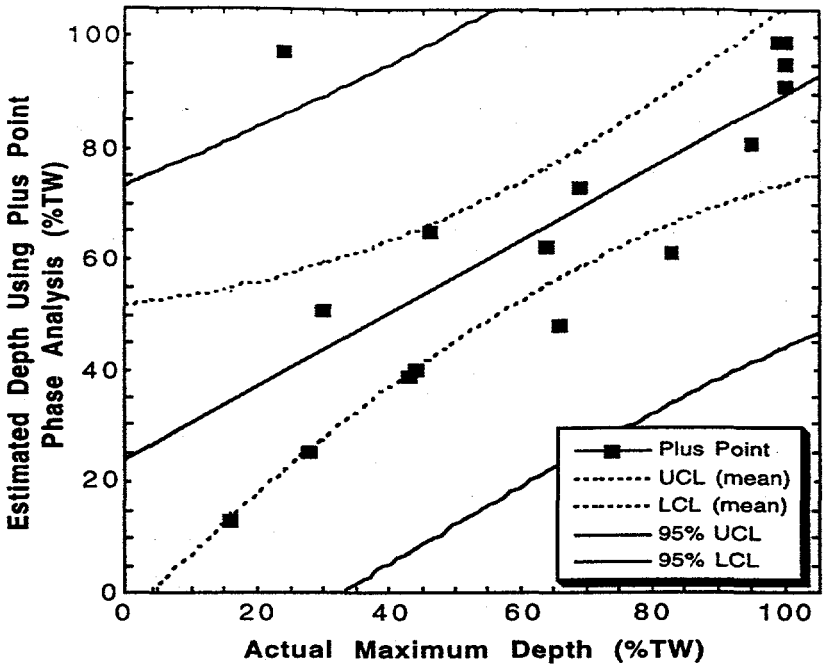

Fig. 8. Depth estimates from Plus Point data with 95% upper and lower confidence limits for mean and additional points. Range of upper and lower confidence limits is very large because of small size of data set.

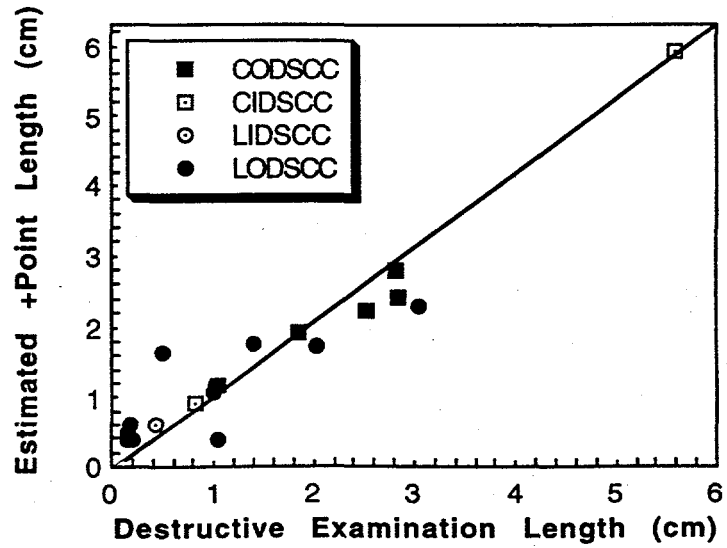

Fig. 9. Estimated crack length vs. destructive examination (DE) from 20-tube set. Estimates were generated from Plus Point eddy current data acquired at Zetec and analyzed at Argonne with Eddynet95 software. For complicated crack structures revealed by DE, full extent of cracking was compared to estimated length. If a well defined deep crack was found among a series of shallow cracks, length of deep crack was compared to eddy-current-determined length.

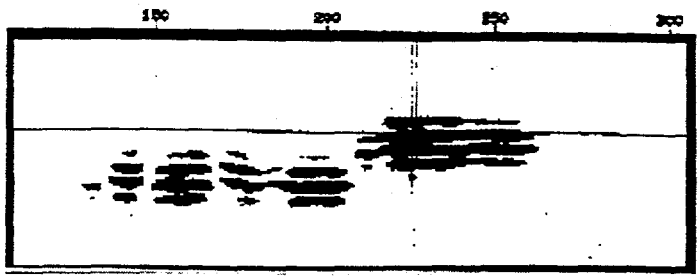

Fig. 10. Ultrasonic Lamb wave image (from ABB-AMDATA) of laboratory grown CODSCC in Inconel 600 SG tube. This image suggests six segments, five at the same axial location and one offset axially with an arc length of 50°. The total arc length indicated ultrasonically is 130°. Destructive analysis showed a crack with total arc length of 160° containing a segment with an arc length of 60° axially offset from the larger segment by about 0.05 in. While destructive examination of lower part of crack shown in this figure does not reveal well-defined segments, the DE does show widely varying depths for this part of crack. Segments indicated ultrasonically are results of low-amplitude signals from shallower parts of continuous crack.

160° and containing a segment with an arc length of 60° axially offset from the larger segment by about 0.05 in. While the destructive examination (DE) of the lower part of the crack shown in this figure does not reveal well-defined segments, the DE does show widely varying depths for this part of the crack. The segments indicated ultrasonically are the result of low-amplitude signals from the shallower parts of the continuous crack.

A second ultrasonic method for characterizing the cracking pattern is the use of high frequency normal-incidence longitudinal waves launched in water. A high-frequency ultrasonic image of an SCC is shown in Fig. 11. The image shows the intersection of a complicated crack with the Inconel 600 tube outer surface. The image shows the roll transition as a horizontal dark line across the center of the image, along with circumferentially and axially oriented crack segments. The axial segments are up to 0.3 in. in extent. A 50-MHz normal-incidence longitudinal focused beam in water was used to create this image (INEL).

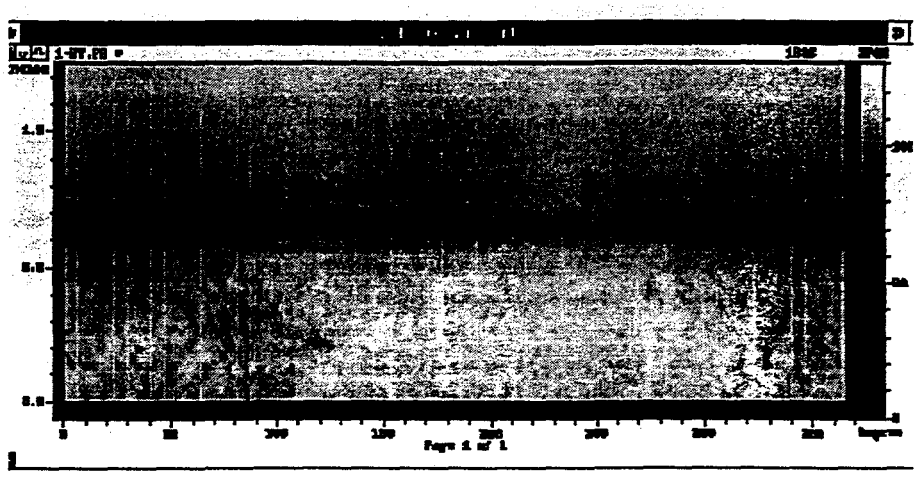

Fig. 11. High-frequency ultrasonic image of an SCC. Image shows intersection of complicated cracks with Inconel 600 tube outer surface. Roll transition appears as a horizontal dark line across center of image, along with circumferentially and axially oriented crack segments. Axial segments are up to 0.3 in. in extent. A 50 MHz normal incidence longitudinal focused beam in water was used to create this image (INEL).

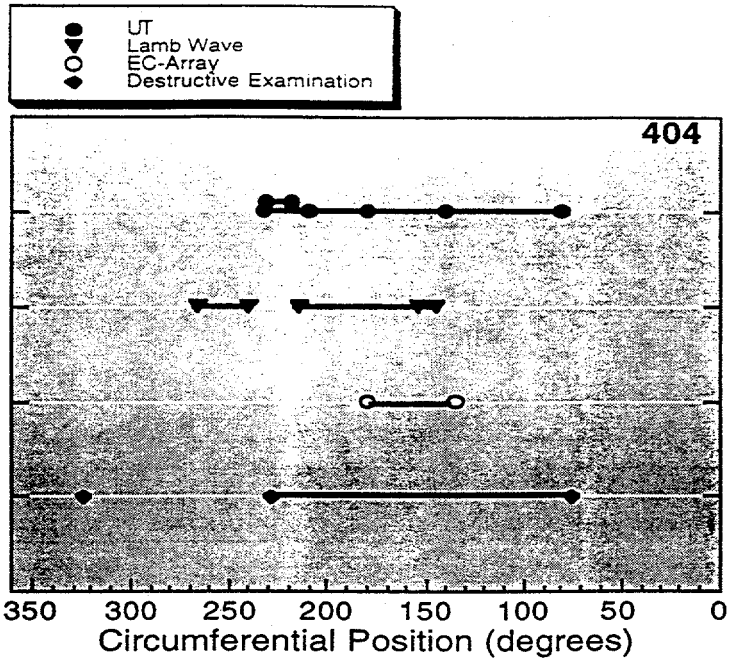

Fig. 13. Predicted length of CIDSCC using high-frequency ultrasonic wave (incident to outer surface of tube) (PNNL/INEL), Lamb wave (ABB), and C5/HD eddy current array (AECL). Symbols between ends of crack representation indicates somewhat segmented structure.

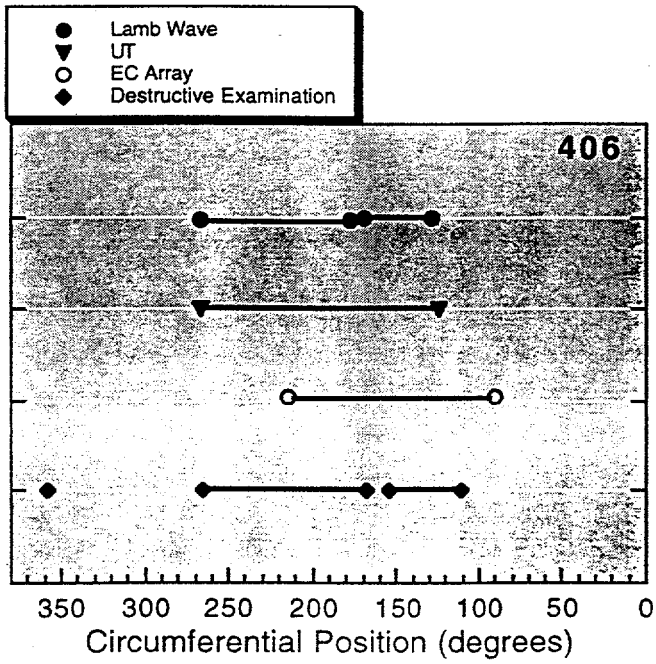

Fig. 14. Predicted length of circumferential ID crack in 22.2-mm (0.875-in.)-diam. Inconel tube using high-frequency ultrasonic wave (incident to outer surface of tube) (PNNL/INEL), Lamb wave (ABB), and C5/HD eddy current array (AECL).

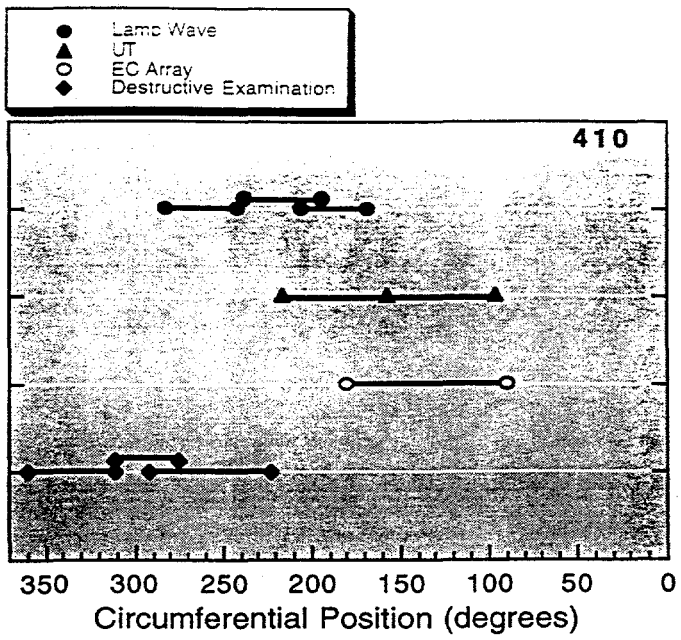

Fig. 15. Comparison of predicted length of circumferential ID crack in 22.2-mm (0.875-in.)-diam. Inconel tube.

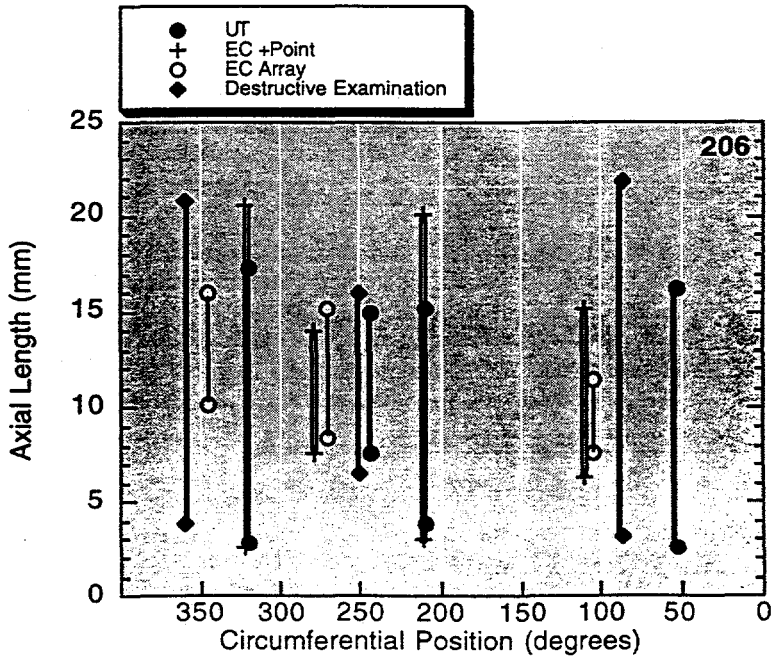

Fig. 16. Predicted length of axial OD crack in 22.2-mm (0.875-in.)-diam. Inconel tube using high-frequency ultrasonic wave (incident to outer surface of tube) (PNNL/INEL), Plus Point probe (ZETEC/ANL), and C5/HD eddy current array (AECL).

Acknowledgments

The authors thank R. Kurtz (PNNL), A. Diaz (PNNL), T. Gomm (INEL), C. Dodd, V. Cecco (Atomic Energy of Canada, Ltd.), M. Brook (ABB AMDATA), and J. Cox (Zetec) for their contributions to the work described in this paper. This work was supported by the Office of Nuclear Regulatory Research, U.S. Nuclear Regulatory Commission.

References

1. C. V. Dodd and J. R. Pate, Advancement in Eddy–Current Test Technology for Steam Generator Tube Inspection, in *Twentieth Water Reactor Safety Information Meeting, NUREG/CP–0126*, Vol. 3, March 1993, pp. 267–276.

2. J. M. Mann, L. W. Schmerr and J. C. Moulder, Neural Network Inversion of Uniform–Field Eddy Current Data, *Mater. Eval.*, Jan. 1991, pp. 34–39.